Evaluation of the role of polyelectrolyte deposition conditions on growth factor release

A.M. Peterson,[a,b]* C. Pilz-Allen,[c] H. Möhwald[b] and D.G. Shchukin[d]

Polyelectrolyte multilayer coatings were prepared from solutions of poly(methacrylic acid) and poly-L-histidine. Bone morphogenetic protein 2 (BMP-2) was adsorbed to the surface of anodized titanium and polyelectrolyte multilayer coatings were built up on top of the BMP-2. The effect of deposition conditions on coating properties and preosteoblast response was measured by comparing coatings prepared under natural conditions to those prepared from solutions at pH = 6.0 and solutions containing 0.1M NaCl. High levels of BMP-2 release were achieved, with coatings prepared from pH = 6.0 solutions releasing 86 ng cm^{-2} and coatings prepared from solutions containing 0.1M NaCl releasing 114 ng cm^{-2} over 25 days. Enhanced preosteoblast differentiation was observed on coatings prepared from modified solutions; however, this increased differentiation was apparent for BMP-2-eluting and control coatings. Additionally, a positive relationship between surface roughness and differentiation was observed, which may account for increased differentiation for systems that do not release BMP-2.

Introduction

As stents, bone scaffolds and hip and other implants become more widely used thanks to longer lifespans in the developed world, it is essential to improve the understanding of biointerfaces and to tailor the surfaces of implanted devices for specific applications. In the United States alone, 1.19 million hip and knee replacements were performed in 2011, a number that has doubled since 1995.[1] Titanium is a popular choice for orthopaedic implant material given its strength, durability, and biocompatibility; however, implant lifetimes are limited because poor interfaces result in implant loosening. Limited integration of an implant with surrounding bone results from poor adhesion and growth of desires cells, either as a result of non-ideal surface properties or adhesion of bacteria and other undesired cells and proteins. Over the past two decades, significant strides have been made in developing improved biointerfaces.[2–5] However, much is still unknown given the complexity of interactions at the implant-body interface.

Polyelectrolytes are polymers that contain ionically dissociable groups. Ions on strong polyelectrolytes are completely dissociated, whereas dissociation is pH-dependent for weak polyelectrolytes. Polyelectrolytes can contain positively (polycation) or negatively (polyanion) charged repeat units. Polyelectrolyte complexes (PECs) can be formed by depositing polycations and polyanions on a surface in an alternating fashion, resulting in a polyelectrolyte multilayer (PEM). PEC films and microcapsules have been used for a variety of applications, including drug delivery,[6–10] microreactors for synthesis of difficult to achieve crystalline nanomaterials,[11–13] direct electron exchange between proteins and electrodes,[14] and encapsulation of corrosion inhibitors for self-healing coatings.[15–17] The properties of a PEM are dependent upon many processing parameters including polyelectrolyte pair, molecular weight,[18–21] deposition pH,[22] salt/electrolyte concentration,[23–28] and number of layers.[29] With this in mind, the properties of the film can be tailored for a given application.

Given the biocompatibility of many polyelectrolytes, polyelectrolyte coatings have been used to improve the biocompatibility of implanted devices. Tryoen-Tóth et al. demonstrated that PEC coatings terminating in poly(styrene sulfonate) (PSS), poly(L-glutamic acid) (PGA) and poly(L-lysine) (PLL) show good biocompatibility for osteoblast-like cells.[30] Schultz et al. later reported a more regular and less obstructed fibroblast layer on PGA-terminated coatings as compared to PLL-terminated coatings. Additionally, by functionalizing the PGA layer with an anti-inflammatory peptide, in vivo production of an anti-inflammatory agent was detected.[31] A PEC coating of hyaluronic acid and chitosan was developed by Chua et al. to confer antibacterial properties.[32] When arginine-glycine-aspartic acid was immobilized on this coating, osteoblast adhesion was also significantly improved as compared to pristine titanium.[33] Additionally, Brunot et al. reported enhanced fibroblast activity on titanium coated with poly(styrene sulfonate)/poly(allylamine hydrochloride) multilayers.[34] Other PEC coatings that have been shown to improve cell adhesion include chitosan/heparin[35] and protamine sulfate/PSS.[36] A number of recent reviews have highlighted the ability of polyelectrolyte multilayers to control cellular function.[9,37–39]

PEMs have also been used on implant surfaces for the controlled release of biologically relevant molecules such as drugs and growth factors. Macdonald et al. demonstrated the coating of a polymer scaffold with LbL-deposited poly(β-aminoester) and chondroitin sulfate, a complex capable of delivering microgram scale amounts of BMP-2.[40] Poly(L-lysine) (PLL)/hyaluronic acid (HA) coatings on a porous ceramic also showed microgram level release of BMP-2 from porous ceramic scaffolds. However, in this case over 60% of release was

observed in the first day. Subsequent studies of the cross-linked PLL/HA coating on titanium surfaces showed cross-link density-dependent release of BMP-2 as well as long term BMP-2 stability (>1 year) when stored at 4°C.[41] Microcapsules made of polyelectrolyte multilayers have also been used for controlled release of biologically relevant molecules.[29,42–44]

Direct comparison of the efficacy of PEM technologies is difficult because of the range of different substrates that have been used, some of which are porous scaffolds. The amount of growth factor release from porous scaffolds is reported per mass or volume of scaffold, while release from planar substrates is measured per surface area and release from microcapsules is related to the concentration of microcapsules. By using the same polyelectrolytes and adjusting processing parameters systematically, we can compare directly to our previous work and begin to describe protein diffusion mechanisms from PEMs where neither hydrolytic degradation nor cross-linking play a role.

Morphogens are biomolecules that act as spatial regulators and dictate cell behaviour and tissue development through concentration gradients. Morphogen gradients can cause cell migration, expression of different genes, and development of different tissues.[45,46] Many morphogens, in particular transcription and growth factors, have been investigated for their ability to control osteoblast outcomes and bone formation.[47–52] One of these, Cbfa1, is an osteoblast-specific transcription factor that is essential for osteoblast differentiation as well as bone formation. Growth factors such as bone morphogenetic proteins (BMPs) have been implicated in Cbfa1 expression, and therefore, osteoblast differentiation.[48] Hughes-Fulford and Li found that BMP-2 plays a critical role in stimulating mineralization.[52] Other studies have confirmed BMP-2's role in enhancing differentiation and extracellular matrix mineralization.[48,51] Therefore, BMP-2 was selected as the growth factor of interest in this study.

The goal of this work is the controlled long term release of BMP-2 from PEM coatings so as to improve osseointegration and durability of titanium implants. Previously, we demonstrated microgram levels of release of a model polypeptide from a PEM coating.[19] That coating was subsequently characterized and release of BMP-2 and basic fibroblast growth factor was achieved. Preosteoblast proliferation and differentiation were enhanced on the BMP-2-eluting coating.[53] The following report investigates the formation, physical properties and preosteoblast response to PEM coatings prepared from modified solutions. In one case, the pH of deposition solutions was adjusted to pH = 6 and in the other example 0.1 M NaCl was added to the solutions. The purpose of this work was to explore the effect of processing conditions on BMP-2 release from and surface properties of a PEM system and then to investigate the effect that these properties have on preosteoblast proliferation and differentiation. While it has long been known that varying solution conditions will affect PEM buildup, this tool has not previously been used for controlled release of growth factors. This report represents a proof of concept for the idea of adjusting BMP-2 release through changing deposition solution conditions.

Experimental

Materials

Titanium foil (99.5% Ti) was acquired from Alfa Aesar. Poly(methacrylic acid, sodium salt) (PMAA, $M_n \approx 5400$, PDI = 1.8), poly-L-histidine hydrochloride (PH, molecular weight ≥ 5000), phosphine buffered saline (PBS, pH = 7.4), α-modified Eagle's medium (α -MEM), gentamicin, ascorbic acid, glucose, bovine serum albumin (BSA), Triton X-100 and ethylenediaminetetraacetic acid (EDTA) were obtained from Sigma-Aldrich. Fetal calf sera and calf sera were obtained from PAA. 4% paraformaldehyde was obtained from BOSTER Biological Technology Ltd. Pronase and Casitron, the measuring buffer for cell counting, were purchased from Roche Diagnostics. Stains Alexa Fluor® 488 and TO-PRO®-3 were purchased from Invitrogen. Recombinant human bone morphogenetic protein 2 (BMP-2), the BMP-2 enzyme linked immune sorbent assay (ELISA) development kits and the ELISA buffer kit were acquired from Peprotech. The DiaSys Diagnostic Systems alkaline phosphatase (ALP) test kit was purchased from Rolf Greiner Biochemica GmbH. MC3T3-E1 pre-osteoblast cells were a gift from Ludwig-Boltzmann-Institute of Osteology.

Titanium preparation

Titanium foil was cleaned in 1.5 M sulphuric acid, then rinsed in deionized water, ethanol, acetone, and again in water. Anodization took place in 165 g L^{-1} sulphuric acid at a potential of 30 V for 5 min. Anodization under these conditions results in a porous oxide structure with pores ranging in size from 40-200 nm in diameter.[19]

Polyelectrolyte multilayer coatings

Coating of titanium foil with the polyelectrolyte complex was achieved by first immersing the anodized titanium specimen in a 0.1 mg mL^{-1} solution of BMP-2 in water for 15 minutes. The polyelectrolyte coating was then formed on top of this adsorbed layer by immersing the plate for 15 minutes in a 1 mg mL^{-1} PMAA in water solution prepared under one of the conditions described below, then in a solution of 1 mg mL^{-1} PH in water for 15 minutes. Specimens were washed three times in water

between each adsorption step to remove weakly adsorbed material. Alternating layers of PMAA and PH were formed until 10 layers (five bilayers) were achieved. Five bilayers were selected because films of this thickness were previously shown to be effective for loading and delivering significantly amounts of BMP-2, basic fibroblast growth factor, and a model polypeptide.[53] As a control for cell culture, polyelectrolyte coatings without BMP-2 were also prepared. For these coatings, PH was adsorbed to anodized titanium as the first step, then five bilayers of PMAA/PH were formed on top of this PH layer. A schematic of the layer-by-layer formation of the PEMs is given in Figure 1

Coatings were prepared under two conditions: 1. Solution pH adjusted to 6.0; 2. 0.1M NaCl added to the deposition solutions. Specimens that were coated with solutions adjusted to pH = 6.0 are denoted as PE-B6 (containing BMP-2) or PE-6 (control without BMP-2). Specimens that were coated with solutions containing 0.1M NaCl are denoted as PE-BN (containing BMP-2) or PE-N. A pH of 6 was selected for two reasons. First, it is below the isoelectric point of BMP-2, meaning that BMP-2 has a net positive charge. However, pH = 6 is also above the pKa of PMAA, so the acid will be mostly dissociated.[19]

The results of this study are compared to previous work in which the polyelectrolyte and BMP-2 solutions were not modified. In this case, solutions of 1 mg mL^{-1} PMAA, 1 mg mL^{-1} PH and 0.1 1 mg mL^{-1} BMP-2 were prepared in DI water. These specimens are described as PE-B and PE for specimens with and without BMP-2, respectively. All PEMs were prepared at 22°C.

Growth factor release

To evaluate release of BMP-2 from PE-B6 and PE-BN coatings, specimens were immersed in PBS. Five specimens were monitored per condition. 1 mL aliquots were taken from the solutions regularly, with the aliquot volume replaced with fresh PBS. Aliquots were promptly frozen at -20 °C. The amount of growth factor released was quantified using enzyme linked immune sorbent assay (ELISA). ELISA was performed in accordance with the instructions provided with the development kit. Aliquots from the release studies were thawed and returned to room temperature immediately prior to their use in the assay.

Cell culture and staining

The MC3T3-E1 preosteoblast cell line was used to evaluate the biocompatibility of coatings. MC3T3-E1 cells were cultured on PE-B6, PE-BN, PE-6, PE-N, and anodized titanium surfaces. PE-6, PE-N and anodized titanium act as controls. Titanium and coated titanium specimens were sterilized using UV light and each specimen was placed in one well of a six well plate. MC3T3-E1 cells were cultured in α-MEM with 4.5 g L^{-1} glucose, 10 vol.% fetal calf sera, 10 µg mL^{-1} Gentamicin and 50 µg mL^{-1} ascorbic acid. Approximately 5.76×10^4 cells per well (6×10^3 cells cm^{-2}) were suspended in culture medium, dispersed over the specimen and cultured for 3, 5, 7, 14 or 21 days in an incubator
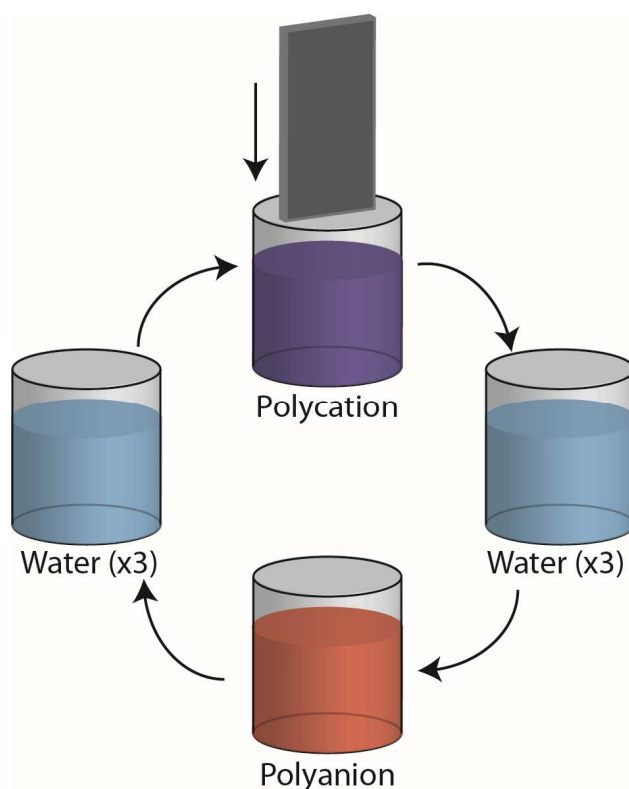

Fig. 1. Schematic of the layer-by-layer formation of PEMs.

(Binder) at 37°C in a humidified atmosphere containing 5% CO_2. Fresh medium was given every 2nd or 3rd day of culture.

Cells cultured for 7 days were stained and imaged with confocal fluorescence microscopy. Cells were fixed for 15 min in 4% paraformaldehyde, washed in PBS, permeabilized with 0.1% Triton X-100 at 4°C for 15 min and washed three times in PBS. F-actin was stained with Alexa Fluor® 488 and cell nuclei were stained with TO-PRO®-3. Confocal micrographs were obtained with a Leica TCS SP confocal scanning system with a 100x oil immersion objective (numerical aperture 1.4).

Cell counting

Cell counting was performed after 3, 5 and 7 days of culture. The titanium specimens with cells were first placed in new six well plates to avoid counting cells on the surface of cell culture wells. Cells on the specimen surface were detached with 500 µL Pronase/EDTA solution (0.001% Pronase/0.02% EDTA in PBS). The detached cells were transferred to 1.5 mL microcentrifuge tubes. The specimens were washed three times with 250 µL PBS. This PBS was also transferred to the microcentrifuge tubes. Cell/Pronase-EDTA/PBS suspensions were then centrifuged at 650 g for 10 min. The supernatant was removed and cells were redispersed in 200 µL PBS. Subsequently, 10 mL of the Casitron solution and 50 µL of the cell suspension were mixed. The number of cells in the resulting liquid were determined with a CASY Model TT cell counter
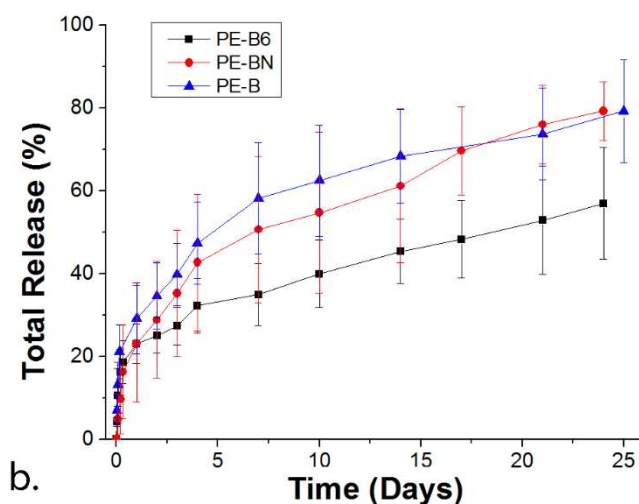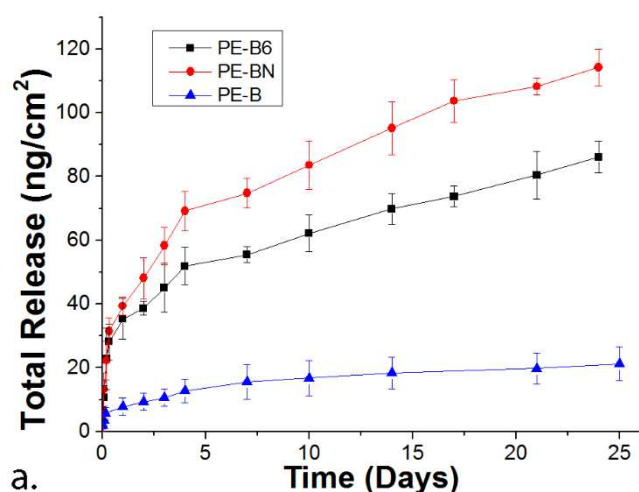
Fig. 2 Amount of BMP-2 release (A) for PE-B6, PE-BN and comparison to PE-B. Percentage of BMP-2 release (B) for PE-B6, PE-BN and comparison to PE-B. Error bars represent standard deviation.

(Roche Diagnostics). Cell counts were performed on three replicates per specimen and three specimens per condition.

Alkaline phosphatase enzyme activity

Preosteoblast differentiation and tissue formation were characterized with alkaline phosphatase (ALP) enzyme activity after 1, 2 and 3 weeks. The cell-seeded titanium surfaces were placed into new wells, washed with PBS, air-dried under laminar airflow for 30 min and frozen at -20°C for 1 h. After freezing, cells were lysed with a 0.5% Triton X-100 solution for 20 min at room temperature. Then, 8 µL or 4 µL of the lysed product was added to 200 µL of the ALP enzyme working reagent. The ALP enzyme working reagent was incubated at 37°C prior to mixing with the lysed product. Immediately after mixing, the absorbance of these samples was measured at 405 nm at 37°C for ten minutes using a plate reader. Results are expressed in units of U L^{-1} and are normalized to a specimen surface area of 1 cm^2. Three specimens were measured for each condition at every time point and the absorbance of these specimens was measured in triplicate.

Coating analysis

Coatings were characterized using scanning electron microscopy (SEM), atomic force microscopy (AFM), contact angle, and quartz crystal microbalance (QCM) analysis. QCM analysis was performed using a Q-Sense instrument on titanium sensors at a flow rate of 50 µl min^{-1} and temperature of 22 °C. Static and dynamic sessile drop methods were used to determine the static contact angles and the advancing and receding contact angles, respectively.

Results and Discussion

BMP-2 release

The release of BMP-2 from PE-B6 and PE-BN is shown in Figure 2. Data from PE-B6 and PE-BN are also compared to data from the unmodified polyelectrolyte multilayer, PE-B.[53] PE-BN is capable of the greatest amount of release, with 114±6 ng cm^{-2} BMP-2 released after 25 days. 86±5 ng cm^{-2} was released from PE-B6 after 25 days. Both of these values are far higher than release from PE-B and are greater than the amount of vascular endothelial growth factor (VEGF) that was immobilized on titanium surfaces by Hu et al.[54] The amount BMP-2 released per time point is shown in Figure 3. For simplicity, all of BMP-2 release within the first day have been combined into one time point.

Similar release behaviour is observed in all systems: high release rate for the first day, medium release rate for days 1-4 and low release rate after day 4. The ratios of high to medium
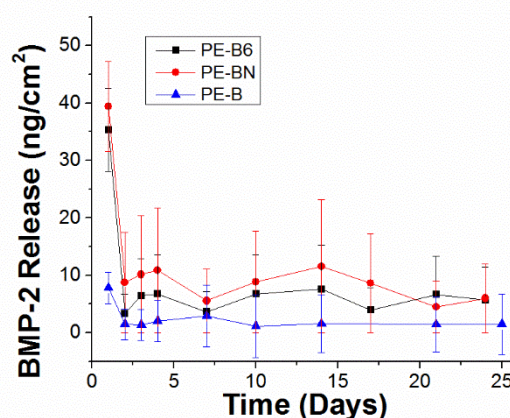
Fig. 3. Amount of BMP-2 release per time point for PE-B6, PE-BN and comparison to PE-B. Error bars represent standard deviation.
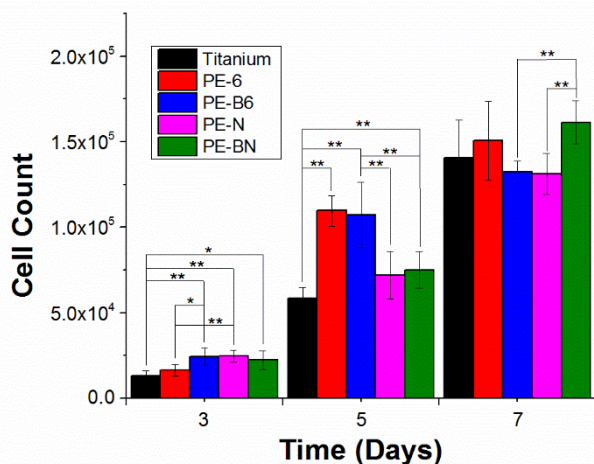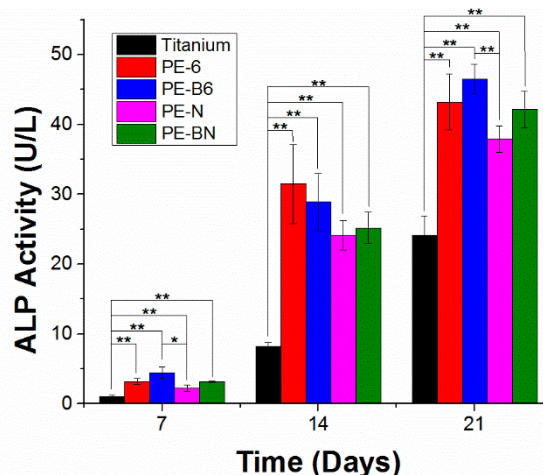
Fig. 4. Cell count over the first week of culture on surfaces prepared from pH = 6 solutions or surfaces prepared from solutions containing 0.1 M NaCl. Cell counts are normalized to a nominal surface area of 1 cm2. Error bars represent standard deviation. * = p < 0.05, ** = p < 0.01.

Fig. 5. ALP enzyme activity on surfaces prepared from pH = 6 solutions and from solutions containing 0.1 M NaCl. ALP enzyme activity values are normalized to a nominal surface area of 1 cm^2. Error bars represent standard deviation. * = p < 0.05, ** = p < 0.01.

release rates range from 8.1 to 14.8, while the ratios of medium to low release rates fall over a smaller range (3.6-5.0). The release profiles follow a $t^{1/2}$ law and are in good agreement ($R^2 >$ 0.95 in all cases) with the Higuchi model.

Further analysis can be performed by comparing percent release, which is shown in Figure 2b. The results from these release studies indicate that all of these films are capable of sustained release. The time for 50% release for PE-B6 and PE-BN are days 17 and 4, respectively. The behaviours of PE-BN and PE-B are identical within error. However, the curve for PE-B6 in Figure 3 deviates from the other two curves after 4 days and is outside of standard deviation after 17 days. Release from PE-BN is therefore identical to that from PE-B and the difference in total mass release results entirely from the amount of BMP-2 that is adsorbed. In this case, BMP-2 exhibits the behaviour of a charged macromolecule and shows increased adsorption under high salt conditions.[28,55–57] The different release behaviour of PE-B6 most likely results from the different polyelectrolyte multilayer structure that is formed from solutions at pH = 6.

Preosteoblast proliferation

The proliferation of preosteoblasts was evaluated on BMP-2-eluting surfaces. The results were compared to preosteoblast proliferation on non-eluting polyelectrolyte coatings and anodized titanium surfaces. Cell count results are summarized in Figure 4. After three days of culture, cells proliferated more on the PE-B6 surfaces than on the two controls (anodized titanium and PE-6, p < 0.01). However, this level of preosteoblast proliferation is statistically equivalent to proliferation on PE-N and PE-BN surfaces. After five days, proliferation on PE-6 and PE-B6 was equivalent and close to twice that of proliferation on anodized titanium. Concerning proliferation on anodized titanium, PE-N and PE-BN surfaces were statistically equivalent after five days. After seven days of culture, there is no

statistically significant effect of the polyelectrolyte coatings or of growth factor release, except in the case of PE-BN. This condition demonstrates greater cell proliferation (p < 0.01) than the control (PE-N) and PE-B6. It is unclear why preosteoblast proliferate more on PE-BN than PE-B6 on day 7, but less on day 5. One explanation could be that by day 7 more preosteoblasts have transitioned from proliferation to differentiation on the PE-B6 surfaces as compared to PE-BN surfaces. Since BMP-2 is primarily implicated in proesteoblast proliferation and the chemistry of all coating surfaces is identical, the observed differences in cell proliferation are most likely the result of differences in surface roughness.[51,52]

After seven days of culture, samples were stained and imaged using confocal fluorescence microscopy. A thick cell layer was observed on all surfaces. These images are provided in the Supporting Information.

Alkaline phosphatase enzyme activity

ALP enzyme activity was used as a marker for preosteoblast differentiation and tissue formation. Results for ALP enzyme activity on different surfaces after one, two and three weeks of culture are given in Figure 5. After one week of culture, the coatings releasing BMP-2 demonstrate significantly higher ALP enzyme activity than their respective control surfaces (p < 0.01). However, after two and three weeks, coatings without BMP-2 show ALP enzyme activity comparable to the BMP-2-releasing coatings.

The enzyme activity on coated surfaces is significantly (p < 0.01) higher than on anodized titanium surfaces. The ALP enzyme activity after three weeks for all coatings is greater than the activity previously reported for the BMP-2-eluting coating prepared from unmodified solutions.[53]

While these values are promising as compared to previous results, it is curious that the increased BMP-2 release did not result in higher ALP enzyme activity for the coatings capable of
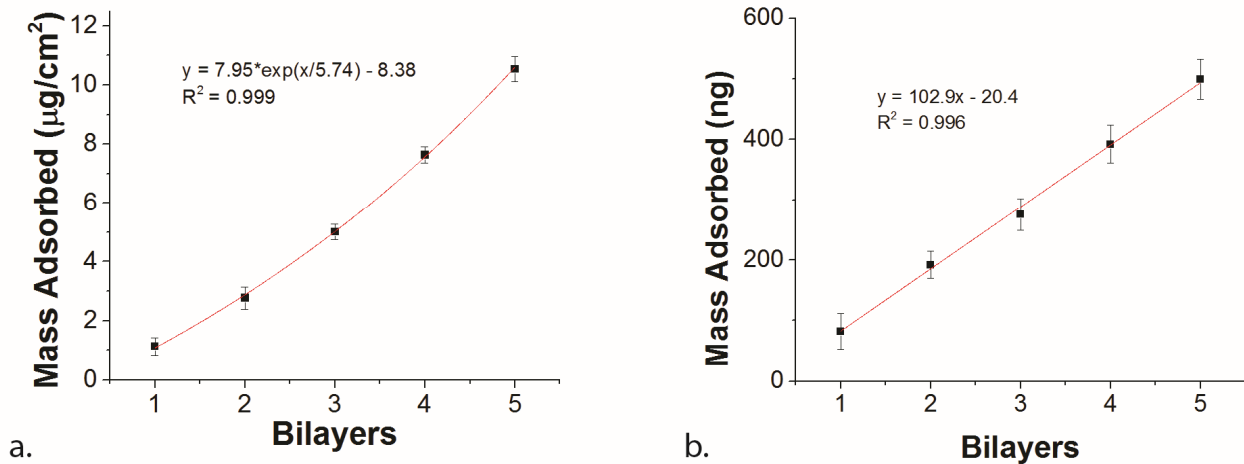
Fig. 6. QCM results for mass adsorbed per bilayer during polyelectrolyte multilayer buildup. (A) Formation of polyelectrolyte multilayer from pH = 6 solutions (PE-6) and (B) solutions containing 0.1 M NaCl (PE-N).

BMP-2 release. As mentioned in the discussion of preosteoblast proliferation, surface roughness most likely plays a role in the observed preosteoblast differentiation and tissue formation.

Coating characterization

QCM was used to quantify the amount of polyelectrolyte that was adsorbed per bilayer during the coating process. Results for PE-6 and PE-N are shown in Figures 6. Non-linear growth of the polyelectrolyte multilayer was observed with PE-6. This is often observed during formation of polyelectrolyte multilayers containing polypeptides such as PH.[58–60] However, linear growth of the polyelectrolyte multilayer was observed for PE-N and was previously reported for the unmodified version of this coating, PE. The masses adsorbed are very close (542 ± 119 vs. 499 ± 33 ng cm^{-2}) for PE and PE-N, while far more is adsorbed for PE-6 (10.5 ± 0.4 μg cm^{-2}).[53] This is a potential explanation for the differences in percentage of BMP-2 release seen in Figure 2b.

Each bilayer of PE-6 is over an order of magnitude thicker than a bilayer of PE-N. However, the difference in BMP-2 release rates is not nearly this large. The main different in release rates occurs in the intermediate time period. There are comparable levels of burst release over the first 24 hours; however, from days 1-4, the rate of release is significantly slower in the thicker case. The greater thickness of the PE-6 coating requires a longer time to diffuse through, resulting in decreased BMP-2 release.

AFM-based surface roughness results are given in Figure 7a. One interesting result is the effect of BMP-2 adsorption on roughness. For the unmodified and pH = 6 condition, adsorbing BMP-2 instead of PH as the first layer has a somewhat significant ($p < 0.10$) effect on root mean squared (RMS) roughness. In the unmodified system, BMP-2 adsorption increases roughness, while in the pH = 6 system BMP-2 adsorption decreases roughness. No difference in roughness was observed for the 0.1M NaCl condition. These differences in effect of BMP-2 adsorption on nanoscale roughness may result from the different
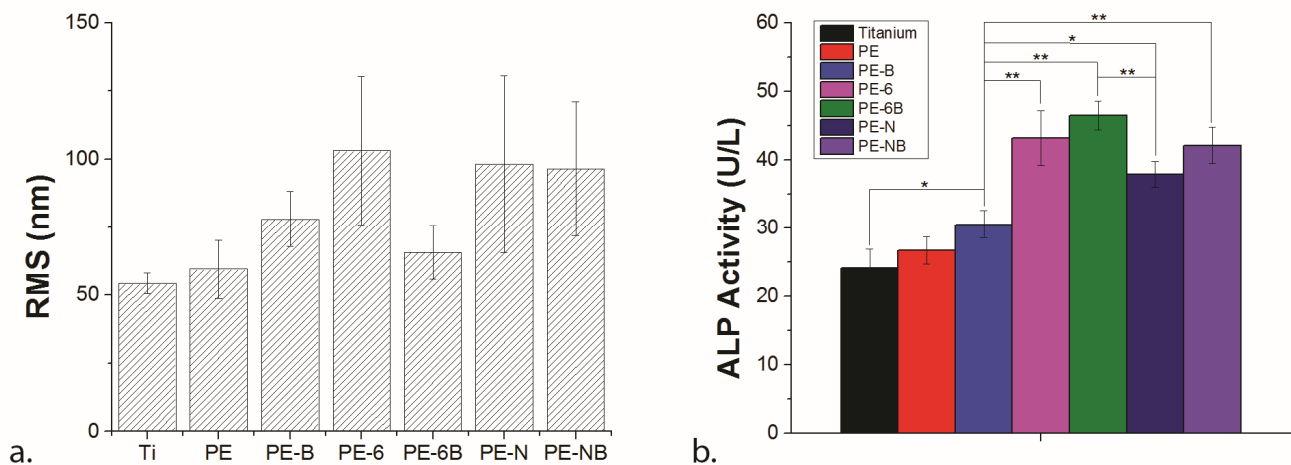

Fig.7. Comparison of (A) surface roughness prior to culture and (B) ALP enzyme activity after 21 days of culture for anodized titanium and polyelectrolyte multilayer-coated anodized titanium surfaces. Error bars represent standard deviation. * = p < 0.05, ** = p < 0.01.

conformations of BMP-2 under the different deposition conditions.

In comparing Figure 7a to Figure 7b, which displays ALP enzyme activity after 21 days of culture, a general trend of increasing ALP enzyme activity with increasing RMS roughness can be observed. The condition that deviates from the trend is PE-6B, which has the second lowest RMS roughness, yet exhibits the highest ALP enzyme activity. In this case, it is possible that the enhanced tissue formation resulting from BMP-2 release is inhibited by low surface roughness.

Static contact angles for all PEM-coated surfaces were on the range of 67-77°, suggesting that the surfaces are chemically similar. The only exception to this is the PE-6 surface, which has a static contact angle of 44.4°. It was also observed that the PE-6 surface absorbed water during the contact angle experiments, so this aberration in contact angle values could be due to bound water in and on the PEM. Contact angle hysteresis for BMP-2 containing coatings is greater than for coatings without BMP-2 (23-30° vs. 15-19°). Therefore, on the microscale, coatings containing BMP-2 are rougher than coatings without BMP-2.[61] SEM micrographs and a table of contact angle values are provided in the Supporting Information. This roughness does not appear to affect preosteoblast differentiation. While SEM micrographs show more debris on the surfaces of coatings without BMP-2, the structure of the coatings containing BMP-2 is rougher and more textured. Microscale roughness differences may result from uneven adsorption and perhaps even agglomeration of BMP-2. Additionally, this uneven adsorption could also impact the nanoscale roughness and is another possible explanation for the differences in roughness observed via AFM.

Conclusions

Polyelectrolyte multilayer coatings were prepared from solutions of PMAA and PH. The effect of deposition conditions on coating properties and preosteoblast response was measured by comparing coatings prepared under natural conditions to those prepared from solutions at pH = 6.0 and solutions containing 0.1M NaCl. This is the first report in which the role of solution conditions on release behaviour and resulting cellular function has been investigated. In this way, surface chemistry was held constant while thickness, polyelectrolyte multilayer structure and surface roughness were varied.

High levels of sustained BMP-2 release can be achieved, with PE-B6 coatings releasing 86 ng cm^{-2} and PE-BN coatings releasing 114 ng cm^{-2} over 25 days. ALP enzyme activity is enhanced on coatings prepared from modified solutions, regardless of their ability to release BMP-2. Additionally, a positive relationship between surface roughness and ALP enzyme activity was observed. Controlling surface roughness and BMP-2 release simultaneously may result in further enhancement of preosteoblast outcomes.

Notes and references

^{a} Department of Chemical Engineering, Worcester Polytechnic Institute, 100 Institute Road, Worcester, MA 01609, United States. Email: ampeterson@wpi.edu
^{b} Department of Interfaces, Max Planck Institute of Colloids and Interfaces, Am Mühlenberg 1, 14476 Potsdam-Golm, Germany
^{c} Department of Biomaterials, Max Planck Institute of Colloids and Interfaces, Am Mühlenberg 1, 14476 Potsdam-Golm, Germany
^{d} Stephenson Institute for Renewable Energy, University of Liverpool, Liverpool L69 3BX, United Kingdom

1. US Department of Health & Human Services, 2013, http://hcupnet.ahrq.gov/HCUPnet.jsp.
2. N. Wisniewski and M. Reichert, *Colloids Surfaces B Biointerfaces*, 2000, **18**, 197–219.
3. M. A. C. Stuart, W. T. S. Huck, J. Genzer, M. Müller, C. Ober, M. Stamm, G. B. Sukhorukov, I. Szleifer, V. V Tsukruk, M. Urban, F. Winnik, S. Zauscher, I. Luzinov, and S. Minko, *Nat. Mater.*, 2010, **9**, 101–113.
4. G. A. Somorjai, H. Frei, and J. Y. Park, *J. Am. Chem. Soc.*, 2009, **131**, 16589–16605.
5. L. Tiefenauer and R. Ros, *Colloids Surfaces B Biointerfaces*, 2002, **23**, 95–114.
6. J. Hong, B.-S. Kim, K. Char, and P. T. Hammond, *Biomacromolecules*, 2011, **12**, 2975–81.
7. E. M. Shchukina and D. G. Shchukin, *Adv. Drug Deliv. Rev.*, 2011, **63**, 837–846.
8. X. R. Teng, D. G. Shchukin, and H. Möhwald, *Langmuir*, 2008, **24**, 383–389.
9. T. Boudou, T. Crouzier, K. Ren, G. Blin, and C. Picart, *Adv. Mater.*, 2010, **22**, 441–467.
10. A. Agarwal, Y. Lvov, R. Sawant, and V. Torchilin, *J. Control. Release*, 2008, **128**, 255–260.
11. D. G. Shchukin, E. Ustinovich, D. V Sviridov, Y. M. Lvov, and G. B. Sukhorukov, *Photochem. Photobiol. Sci.*, 2003, **2**, 975–977.
12. D. G. Shchukin and G. B. Sukhorukov, *Langmuir*, 2003, **19**, 4427–4431.
13. D. G. Shchukin, G. B. Sukhorukov, and H. Möhwald, *J. Phys. Chem. B*, 2004, **108**, 19109–19113.
14. J. Kong, Z. Lu, Y. M. Lvov, R. Z. B. Desamero, H. A. Frank, and J. F. Rusling, *J. Am. Chem. Soc.*, 1998, **120**, 7371–7372.
15. S. V. Lamaka, D. G. Shchukin, D. V. Andreeva, M. L. Zheludkevich, H. Möhwald, and M. G. S. Ferreira, *Adv. Funct. Mater.*, 2008, **18**, 3137–3147.
16. D. O. Grigoriev, K. Köhler, E. Skorb, D. G. Shchukin, and H. Möhwald, *Soft Matter*, 2009, **5**, 1426–1432.
17. D. V Andreeva, D. Fix, H. Möhwald, and D. G. Shchukin, *Adv. Mater.*, 2008, **20**, 2789–2794.
18. T. Mauser, C. Déjugnat, H. Möhwald, and G. B. Sukhorukov, *Langmuir*, 2006, **22**, 5888–5893.

19. A. M. Peterson, H. Möhwald, and D. G. Shchukin, *Biomacromolecules*, 2012, **13**, 3120–3126.

20. L. Shen, P. Chaudouet, J. Ji, and C. Picart, *Biomacromolecules*, 2011, **12**, 1322–1331.

21. C. Porcel, P. Lavalle, G. Decher, B. Senger, J.-C. Voegel, and P. Schaaf, *Langmuir*, 2007, **23**, 1898–1904.

22. A. A. Antipov, G. B. Sukhorukov, S. Leporatti, I. L. Radtchenko, E. Donath, and H. Möhwald, *Colloids Surfaces A Physicochem. Eng. Asp.*, 2002, **198-200**, 535–541.

23. S. T. Dubas and J. B. Schlenoff, *Langmuir*, 2001, **17**, 7725–7727.

24. O. V. Lebedeva, B.-S. Kim, K. Vasilev, and O. I. Vinogradova, *J. Colloid Interface Sci.*, 2005, **284**, 455–462.

25. H. W. Jomaa and J. B. Schlenoff, *Macromolecules*, 2005, **38**, 8473–8480.

26. R. A. McAloney, V. Dudnik, and M. C. Goh, *Langmuir*, 2003, **19**, 3947–3952.

27. R. A. Ghostine, R. M. Jisr, A. Lehaf, and J. B. Schlenoff, *Langmuir*, 2013, **29**, 11742–11750.

28. S. T. Dubas and J. B. Schlenoff, *Macromolecules*, 1999, **32**, 8153–8160.

29. A. A. Antipov, G. B. Sukhorukov, E. Donath, and H. Möhwald, *J. Phys. Chem. B*, 2001, **105**, 2281–2284.

30. P. Tryoen-Tóth, D. Vautier, Y. Haikel, J.-C. Voegel, P. Schaaf, J. Chluba, and J. Ogier, *J. Biomed. Mater. Res.*, 2002, **60**, 657–667.

31. P. Schultz, D. Vautier, L. Richert, N. Jessel, Y. Haikel, P. Schaaf, J.-C. Voegel, J. Ogier, and C. Debry, *Biomaterials*, 2005, **26**, 2621–2630.

32. P. H. Chua, K. G. Neoh, Z. Shi, and E. T. Kang, *J. Biomed. Mater. Res. Part A*, 2008, **87**, 1061–1074.

33. P.-H. Chua, K.-G. Neoh, E.-T. Kang, and W. Wang, *Biomaterials*, 2008, **29**, 1412–1421.

34. C. Brunot, B. Grosgogeat, C. Picart, C. Lagneau, N. Jaffrezic-Renault, and L. Ponsonnet, *Dent. Mater.*, 2008, **24**, 1025–1035.

35. S. Schweizer, T. Schuster, M. Junginger, G. Siekmeyer, and A. Taubert, *Macromol. Mater. Eng.*, 2010, **295**, 535–543.

36. R. E. Samuel, A. Shukla, D. H. Paik, M. X. Wang, J. C. Fang, D. J. Schmidt, and P. T. Hammond, *Biomaterials*, 2011, **32**, 7491–7502.

37. C. J. Detzel, A. L. Larkin, and P. Rajagopalan, *Tissue Eng. Part B Rev.*, 2011, **17**, 101–113.

38. R. F. Fakhrullin, A. I. Zamaleeva, R. T. Minullina, S. A. Konnova, and V. N. Paunov, *Chem. Soc. Rev.*, 2012, **41**, 4189–4206.

39. R. F. Fakhrullin and Y. M. Lvov, *ACS Nano*, 2012, **6**, 4557–4564.

40. M. L. Macdonald, R. E. Samuel, N. J. Shah, R. F. Padera, Y. M. Beben, and P. T. Hammond, *Biomaterials*, 2011, **32**, 1446–1453.

41. R. Guillot, F. Gilde, P. Becquart, F. Sailhan, A. Lapeyrere, D. Logeart-Avramoglou, and C. Picart, *Biomaterials*, 2013, **34**, 5737–5746.

42. K. Sato, K. Yoshida, S. Takahashi, and J. Anzai, *Adv. Drug Deliv. Rev.*, 2011, **63**, 809–821.

43. G. B. Sukhorukov, A. L. Rogach, B. Zebli, T. Liedl, A. G. Skirtach, K. Köhler, A. A. Antipov, N. Gaponik, A. S. Susha, M. Winterhalter, and W. J. Parak, *Small*, 2005, **1**, 194–200.

44. Z. She, M. N. Antipina, J. Li, and G. B. Sukhorukov, *Biomacromolecules*, 2010, 11, 1241–1247.

45. M. B. O'Connor, D. Umulis, H. G. Othmer, and S. S. Blair, *Development*, 2006, **133**, 183–193.

46. P. V Gordon, C. Sample, A. M. Berezhkovskii, C. B. Muratov, and S. Y. Shvartsman, *Proc. Natl. Acad. Sci. U. S. A.*, 2011, **108**, 6157–6162.

47. C. H. Thomas, J. H. Collier, C. S. Sfeir, and K. E. Healy, *Proc. Natl. Acad. Sci. U. S. A.*, 2002, **99**, 1972–1977.

48. C. A. Luppen, E. Smith, L. Spevak, A. L. Boskey, and B. Frenkel, *J. Bone Miner. Res.*, 2003, **18**, 1186–1197.

49. J. Y. Lee, Z. Qu-Petersen, B. Cao, S. Kimura, R. Jankowski, J. Cummins, A. Usas, C. Gates, P. Robbins, A. Wernig, and J. Huard, *J. Cell Biol.*, 2000, **150**, 1085–1100.

50. J. E. M. Brouwers, C. C. van Donkelaar, B. G. Sengers, and R. Huiskes, *J. Biomech.*, 2006, **39**, 2774–2782.

51. G. Rawadi, B. Vayssière, F. Dunn, R. Baron, and S. Roman-Roman, *J. Bone Miner. Res.*, 2003, **18**, 1842–1853.

52. M. Hughes-Fulford and C.-F. Li, *J. Orthop. Surg. Res.*, 2011, **6**, 8.

53. A. M. Peterson, C. Pilz-Allen, T. Kolesnikova, H. Möhwald, and D. G. Shchukin, *ACS Appl. Mater. Interfaces*, dx.doi.org/10.1021/am404849y.

54. X. Hu, K.-G. Neoh, Z. Shi, E.-T. Kang, C. Poh, and W. Wang, *Biomaterials*, 2010, **31**, 8854–8863.

55. G. Decher, J. D. Hong, and J. Schmitt, *Thin Solid Films*, 1992, **210-211**, 831–835.

56. G. Decher, *Science*, 1997, **277**, 1232–1237.

57. J. B. Schlenoff and S. T. Dubas, *Macromolecules*, 2001, **34**, 592–598.

58. C. Porcel, P. Lavalle, V. Ball, G. Decher, B. Senger, J.-C. Voegel, and P. Schaaf, *Langmuir*, 2006, **22**, 4376–4383.

59. C. Picart, J. Mutterer, L. Richert, Y. Luo, G. D. Prestwich, P. Schaaf, J.-C. Voegel, and P. Lavalle, *Proc. Natl. Acad. Sci. U. S. A.*, 2002, **99**, 12531–12535.

60. J. M. Garza, P. Schaaf, S. Muller, V. Ball, J. F. Stoltz, J.-C. Voegel, and P. Lavalle, *Langmuir*, 2004, **20**, 7298–7302.

61. H. B. Eral, D. J. C. M. 't Mannetje, and J. M. Oh, *Colloid Polym. Sci.*, 2012, **291**, 247–260.